

# Effects of Gamma Radiation on Charge-Coupled Devices

D. F. Barbe

J. M. Killiany

H. L. Hughes

Naval Research Lab.  
Washington, D. C.

Naval Research Lab.  
Washington, D. C.

Naval Research Lab.  
Washington, D. C.

**ABSTRACT.** The effects of ionizing radiation (gamma) on the operation of two-phase stepped-oxide surface-channel charge-coupled devices were studied. For total doses up to  $10^5$  rads (Si), the primary cause of changes in CCD operation is a negative shift in the flatband voltage, with the flatband-voltage shift for the polysilicon electrodes being greater than that for the aluminum electrodes. For fixed applied voltages, the flatband-voltage shifts cause: (1) an increase in transfer inefficiency due to the cutoff of Fat Zero, and (2) a decrease in the full-well capacity due to the modified surface potential profile. Up to  $10^5$  rads, the pre-irradiation transfer inefficiency could be recovered by changing the input-gate voltage to compensate for the flatband-voltage shift. Up to  $10^5$  rads, no significant effects due to radiation-induced interface states were observed; however, at  $3 \times 10^5$  rads increases in transfer inefficiency and dark current attributed to radiation-induced interface states were observed.

## INTRODUCTION

Since many applications of charge coupled devices (CCD's) involve radiation environments, a study of the effects of ionizing radiation on the devices is important. In this paper we discuss the effect of gamma radiation on the transfer inefficiency, full-well capacity, and dark current of two-phase, stepped-oxide surface channel CCD's.

## EXPERIMENTAL DETAILS

The test structure employed is shown in Fig. 1. The substrate was 1 ohm-cm N-type silicon with  $\langle 100 \rangle$  orientation. The channel oxide was steam grown  $\text{SiO}_2$ ,  $1000\text{\AA}$  thick under the polysilicon electrodes and  $2400\text{\AA}$  thick under the aluminum electrodes. The channel width was 5 mils.<sup>1</sup> The particular  $\text{SiO}_2$  growth process was chosen to give a low interface state density, and no attempt was made to optimize the radiation hardness.

The circuit used for the testing is also shown in Fig. 1. The input signal and Fat Zero<sup>2</sup> are introduced into the shift register by controlling the source potential  $E_S$ , the input gate bias  $E_{G-S}$ , and the pulse amplitude  $V_{IN}$ . The phase voltage clocks  $\phi-1$  and  $\phi-2$  swing from ground to -10 volts;  $\phi-1$  is -10

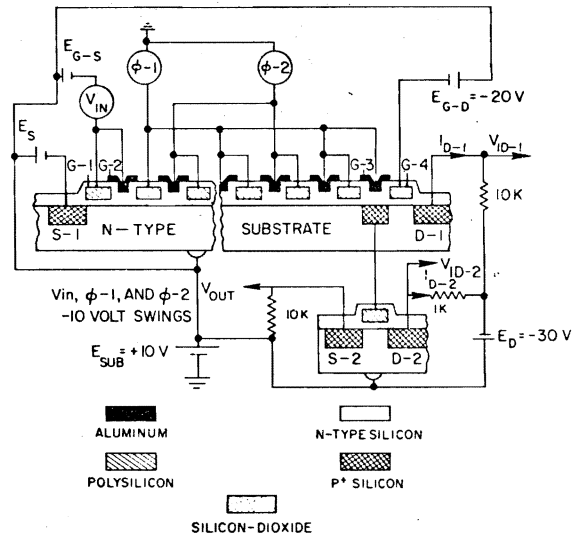


Figure 1. Schematic diagram showing the CCD structure and the circuit configurations

volts while  $\phi-2$  is at ground and vice versa. Both phases are at -10 volts for slightly more than half the period. The first output gate G-3 is connected to  $\phi-1$ , and the second

output gate G-4 is biased to a voltage  $E_{G-D}$  (-20 volts) which is less negative than the drain bias  $E_D$  (-30 volts). The output signal can be sensed directly as current  $I_{D-1}$  or as current  $I_{D-2}$ . The substrate is biased at  $E_{SUB}$  (+10 volts) with respect to ground.<sup>3</sup>

Eight 64-bit CCD's were studied, and four of these devices were irradiated through the complete sequence of  $10^4$ ,  $5 \times 10^4$ ,  $10^5$ , and  $3 \times 10^5$  rads (Si) using a Cobalt-60 gamma source. During the irradiation, the devices were operated as shift registers clocked at 1 MHz with bias settings to give a transfer inefficiency,  $\epsilon$ , of  $10^{-4}$  ( $E_S = -1V$ ,  $E_{G-S} \sim -6V$ ). Up to  $10^5$  rads the dose rate was  $6 \times 10^3$  rads/min, above  $10^5$  rads the dose rate was  $3 \times 10^4$  rads/min. The changes in flatband voltage,  $\Delta V_{FB}$ , for the polysilicon and aluminum electrodes were determined from 1 MHz C-V measurements; the fast interface-state densities were determined from C-V measurements and also by the double pulse technique described in Ref. 4; the dark current was determined from  $I_{D-1}$  measurements; and the transfer inefficiency,  $\epsilon$ , was determined from the loss in a burst of 6 pulses applied at intervals of 80 clock periods

$$\epsilon = \frac{\sum \text{fractional losses in leading pulses}}{\text{total number of transfers}} \quad (1)$$

Typical waveforms obtained for 64-bit devices are shown in Fig. 2

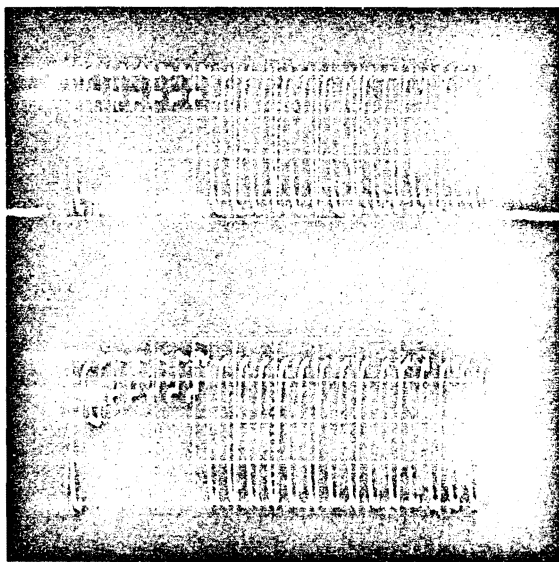


Figure 2. Oscilloscopes of  $V_{OUT}$ . (upper)  $\epsilon = 10^{-4}$  with 20% Fat Zero. (lower)  $\epsilon = 2.3 \times 10^{-3}$  no Fat Zero.

## EXPERIMENTAL RESULTS AND DISCUSSION

The flatband-voltage shifts for the polysilicon and aluminum electrodes shown in Fig. 3 have two major effects on CCD operation: (1) the fact that  $\Delta V_{FB}$  for the polysilicon electrodes is greater than  $\Delta V_{FB}$  for the aluminum electrodes causes the surface-potential profile to change as shown in Fig. 4, thereby reducing the full-well capacity.

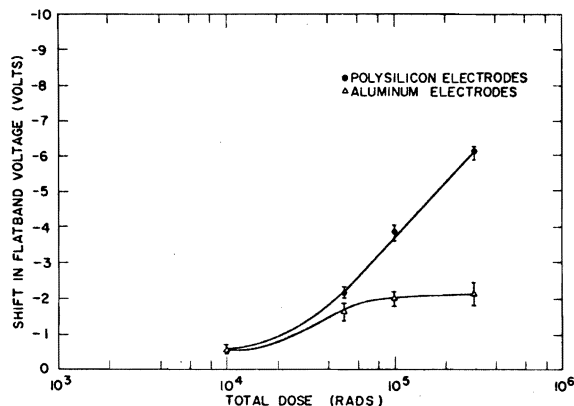


Figure 3. Average flatband voltage shift vs. total dose for polysilicon electrodes and for aluminum electrodes.

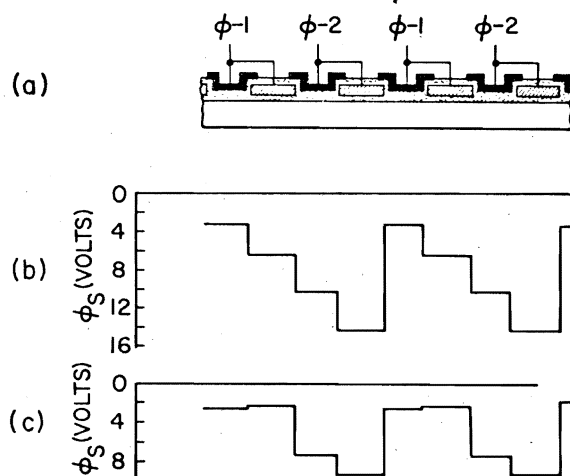


Figure 4. CCD structure and surface potential profiles for  $\phi-1 = -10V$ ,  $\phi-2 = -20V$ ; (a) cross section of CCD structure; (b) pre-irradiation surface potential profile; (c) surface potential profile after  $3 \times 10^5$  rads.

The surface potential profiles were calculated using flatband voltages obtained from C-V measurements and the equation<sup>5</sup>

$$V_G - V_{FB} = \phi_S + (2\epsilon_s q N \phi_S)^{1/2} / C_o, \quad (2)$$

where

$V_G$  = voltage applied to the electrode with respect to the substrate,

$\epsilon_s$  = semiconductor dielectric constant,

$q = 1.6 \times 10^{-19}$  coulomb,

$N$  = doping density of the substrate, and

$C_o$  = oxide capacitance per unit area.

The flatband-voltage,  $V_{FB}$ , is given by

$$V_{FB} = \phi_{MS} - \frac{1}{C_o d} \int_0^d x \rho(x) dx \quad (3)$$

where

$\phi_{MS}$  = the metal-semiconductor contact potential difference,

$\rho(x)$  = the volume charge density in the insulator, and

$d$  = thickness of the insulator.

Solving equation (2) for the surface potential  $\phi_S$  gives

$$\phi_S = V_o + V - (V_o^2 + 2 V V_o)^{1/2}, \quad (4)$$

where  $V = V_G - V_{FB}$ , and

$$V_o = \frac{\epsilon_s q N}{C_o^2}$$

At  $3 \times 10^5$  rads, the measured full-well capacity was 20% of the pre-irradiation capacity; the calculation based on flatband-voltage shifts gives 22%. For larger doses, this effect could cause the loss of charge transfer directionality. (2) The curves of  $\epsilon$  vs dose shown in Fig. 5 can be interpreted in terms of the known effect of radiation of the input gate; i.e., the  $\Delta V_{FB}$  for the aluminum electrode tends to cut off the input gate thereby reducing both the Fat Zero input and the signal input. The initial steep rise in  $\epsilon$  for the device operating at constant voltages set for a 20% pre-irradiation Fat Zero (dots), is due to the cutoff of Fat Zero. For doses above  $10^4$  rads, the transfer loss was nearly constant, independent of amount of charge in the packets. The amount of charge in the input pulses decreased with increasing dose because of the flatband-voltage shift for the input gate; therefore,  $\epsilon$  gradually increased with increasing dose. The straight line (squares) represents  $\epsilon$  vs. dose with no Fat Zero being introduced through the input gate

and with  $V_{IN}$  adjusted after each dose so that the input charge packets fill the wells. The gradual increase in  $\epsilon$  for increasing dose is due to the decrease in full-well capacity since the loss is nearly independent of the amount of signal charge. Up to  $10^5$  rads,  $\epsilon = 10^{-4}$  was recovered by increasing the input-gate voltage ( $\leq 1$  V) to compensate for  $\Delta V_{FB}$  and restore the Fat Zero to  $\sim 20\%$  of a pre-irradiation full well (circles).

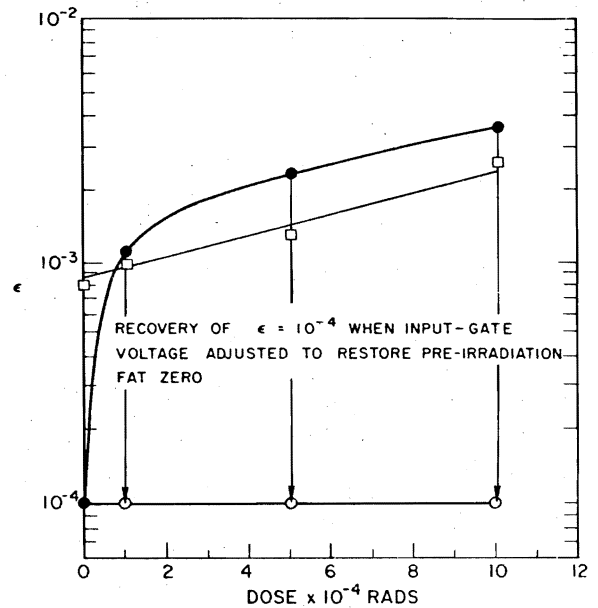


Figure 5. Transfer inefficiency vs. total dose: (dots) Pre-irradiation Fat Zero = 20%, all applied voltages held constant; (squares) No input Fat Zero,  $V_{IN}$  adjusted after each dose for full well input bursts; (circles) Input gate bias voltage adjusted after each dose to restore pre-irradiation Fat Zero, thereby recovering pre-irradiation  $\epsilon$ .

The mechanisms responsible for  $\epsilon$  vs. dose effects are summarized in Table 1.

The double pulse measurement was performed by clocking bursts of 16 "ones" separated by a string of "zeros" through the device. The change in  $\epsilon$  caused by increasing the number of "zeros" between ones when the device was operated without any intentionally introduced Fat Zero is shown in Fig. 6.

Table 1

Mechanisms Responsible for  $\epsilon$  vs. Dose Effects

Experimental Conditions	0 · 10 <sup>4</sup> Rads	10 <sup>4</sup> · 10 <sup>5</sup> Rads
Pre-irradiation Fat Zero = 20%; all applied voltage held constant (Dots)	Fat Zero cutoff due to $\Delta V_{FB}$ for input gate	Loss nearly independent of amount of input charge; decreasing input charge due to $\Delta V_{FB}$ for input gate.
No input Fat Zero; $V_{IN}$ adjusted after each dose for full-well input bursts (Squares)	Loss nearly independent of amount of input charge; decreasing input charge due to decreasing full-well capacity.	

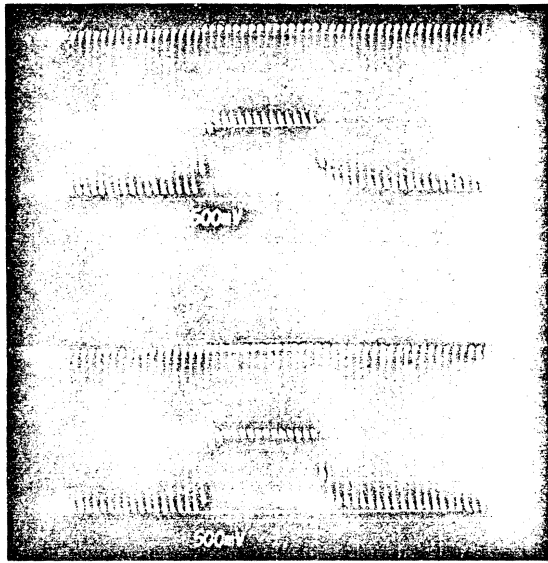


Figure 6. Oscilloscopes of  $V_{OUT}$ . (upper) Bursts of ones separated by 112 zeros. (lower) Burst of ones separated by 250 zeros.

The relationship between transfer inefficiency and interface-state density  $N_{ss}$  is given by<sup>4</sup>

$$\epsilon = \frac{kTN_{ss}}{N_{sig}} \ln(M n_{zero}), \quad (5)$$

where  $k$  = Boltzmann's constant,  
 $T$  = temperature,  
 $M$  = number of phase electrodes per bit,  
 $n_{zero}$  = number of zeros between bursts of ones, and  
 $N_{sig}$  = number of charge carriers per  $cm^2$  in the signal packet.

The fast interface-state densities measured by the double-pulse technique were  $\sim 10^{10}$

$cm^{-2}(eV)^{-1}$  for non-irradiated devices and  $\sim 5 \times 10^{10} cm^{-2}(eV)^{-1}$  after  $3 \times 10^5$  rads.

The interface state densities were also determined by means of C-V measurements. The Gray-Brown technique<sup>6</sup> was employed at zero rads, giving  $\sim 10^{10} cm^{-2}$  for both the aluminum and polysilicon gates. The Lehoc<sup>7</sup> method was used on the irradiated devices giving interface state densities of  $2 \times 10^{11} cm^{-2}$  for the aluminum gates and  $5 \times 10^{11} cm^{-2}$  for the polysilicon gates at  $3 \times 10^5$  rads. The interface state measurements are summarized in Table 2.

Table 2

Fast Interface-State Densities Before and After Irradiation as Measured by C-V and Double Pulse Techniques

Measurement Technique	Units	Unirradiated		After $3 \times 10^5$ Rads	
		Polysilicon Electrodes	Aluminum Electrodes	Polysilicon Electrodes	Aluminum Electrodes
C-V	$cm^{-2}$	$10^{10}$	$10^{10}$	$5 \times 10^{11}$	$2 \times 10^{11}$
Double Pulse	$(cm^2 eV)^{-1}$	$10^{10}$		$5 \times 10^{10}$	

The C-V measurements were made by connecting all of the CCD electrodes of one type (aluminum or polysilicon) together. Before irradiation slight undulations were observed in the C-V curves for the polysilicon electrodes. The undulations became more pronounced with increasing dose, indicative of non-uniform  $\Delta V_{FB}$  from one polysilicon electrode to the next.

At  $3 \times 10^5$  rads, CCD operation with pre-irradiation voltages was seriously degraded. This was due to the loss of full-well capacity, input-gate cutoff, and increased interface trapping. With bias adjustments to compensate for the flatband voltage shifts shown in Fig. 3,  $\epsilon = 8 \times 10^{-4}$  was measured with a Fat Zero of 20% of a pre-irradiation full well, and 60% of the pre-irradiation full-well capacity was recovered. Since the full-well capacity of the overall device is determined by the cell having the least capacity in the device, nonuniform radiation induced  $\Delta V_{FB}$  is the probable reason that the pre-irradiation full-well capacity was not fully recovered.

The dark current was measured by continuously clocking the CCD at 1 MHz with the

device shielded from light, and measuring the output current with an electrometer. The pre-irradiation dark current<sup>3</sup> was  $\sim 1000$  na/cm<sup>2</sup>. After  $3 \times 10^5$  rads the dark current was  $\sim 3000$  na/cm<sup>2</sup> with the electrode biases adjusted to compensate for  $\Delta V_{FB}$ ; i.e., equal depletion volume. The CCD's tested had many dark current spikes. A typical dark current profile is shown in Fig. 7.

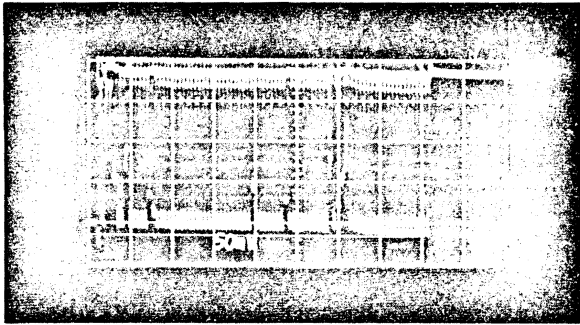


Figure 7. Oscillograph of  $V_{OUT}$  with the device shielded from room light. Integration time = 30 msec,  $E_0 = -10v$ .

Devices of this type without spikes usually have dark current densities of  $50$  na/cm<sup>2</sup>.<sup>3</sup>

#### CONCLUSIONS

It is concluded that for radiation doses up to  $10^5$  rads, the primary cause of changes in two-phase stepped-oxide CCD operation is a negative shift in flatband voltage. For fixed applied voltages, this results in an increase in transfer inefficiency due to Fat Zero reduction and a loss in full-well capacity due to the modified potential-well profile. The pre-irradiation  $\epsilon = 10^{-4}$  can be recovered by increasing the input-gate bias to compensate for flatband-voltage shifts. This, of course, suggests that a MOS transistor to sense  $\Delta V_{FB}$  could be used in a feedback loop to electronically correct the gate voltage for  $\Delta V_{FB}$ . Up to  $10^5$  rads, no significant effects due to radiation-induced interface states were observed; however, at  $3 \times 10^5$  rads increases in  $\epsilon$  (x8) and dark-current density (x3) were measured.

#### BIBLIOGRAPHY

1. The devices were fabricated by RCA Laboratories, Princeton, N. J.
2. "Fat Zero" is the term commonly used to describe a background charge introduced into all potential wells.

3. W. F. Kosonocky and J. E. Carnes, RCA Review 34, 164 (1973)

4. J. E. Carnes and W. F. Kosonocky, Appl. Phys. Lett. 20, 261 (1972)

5. G. F. Amelio, W. J. Bertram, Jr., and M. F. Tompsett, IEEE Trans. on Electron Devices ED-18, 986 (1971)

6. P. V. Gray and D. M. Brown, Appl. Phys. Lett. 8, 31 (1966)

7. K. Lehovec and A. Slobodskoy, Solid State Electronics 7, 59 (1964)

REVERSE SIDE BLANK